SCIENTIFIC REPORTS

OPEN

SUBJECT AREAS:
BEHAVIOUR
GENETIC POLYMORPHISM
NEUROANATOMY
NEURODEVELOPMENTAL DISORDERS

Received
18 April 2011

Accepted
23 May 2011

Published
17 June 2011

Correspondence and requests for materials should be addressed to J.A. (jaruga@brain.riken.jp)

* These authors contributed equally to this work.

‡ Present address: Division of Molecular Biology, Institute of Medical Science, The University of Tokyo, Minato-ku, Tokyo 108-8639, Japan.

Zic2 hypomorphic mutant mice as a schizophrenia model and *ZIC2* mutations identified in schizophrenia patients

Minoru Hatayama[1]*, Akira Ishiguro[1]*‡, Yoshimi Iwayama[2], Noriko Takashima[1], Kazuto Sakoori[1], Tomoko Toyota[2], Yayoi Nozaki[1], Yuri S. Odaka[1], Kazuyuki Yamada[3], Takeo Yoshikawa[2] & Jun Aruga[1]

[1]Laboratory for Behavioral and Developmental Disorders, [2]Laboratory for Molecular Psychiatry, and [3]Support Unit for Animal Experiments, RIKEN Brain Science Institute, Wako-shi, Saitama 351-0198, Japan.

***ZIC2* is a causal gene for holoprosencephaly and encodes a zinc-finger-type transcriptional regulator. We characterized *Zic2*$^{kd/+}$ mice with a moderate (40%) reduction in *Zic2* expression. *Zic2*$^{kd/+}$ mice showed increased locomotor activity in novel environments, cognitive and sensorimotor gating dysfunctions, and social behavioral abnormalities. *Zic2*$^{kd/+}$ brain involved enlargement of the lateral ventricle, thinning of the cerebral cortex and corpus callosum, and decreased number of cholinergic neurons in the basal forebrain. Because these features are reminiscent of schizophrenia, we examined *ZIC2* variant-carrying allele frequencies in schizophrenia patients and in controls in the Japanese population. Among three novel missense mutations in ZIC2, R409P was only found in schizophrenia patients, and was located in a strongly conserved position of the zinc finger domain. Mouse Zic2 with the corresponding mutation showed lowered transcription-activating capacity and had impaired target DNA-binding and co-factor-binding capacities. These results warrant further study of ZIC2 in the pathogenesis of schizophrenia.**

Zic2/ZIC2 is a member of the Zic family of zinc finger proteins, which function as transcriptional regulators with critical roles in neural development[1–5]. In humans, haploinsufficiency of *ZIC2* results in holoprosencephaly (HPE)[6,7] in which the formation of medial forebrain structures is disturbed. *ZIC2* mutations are found in 3%–4% of unrelated individuals with isolated HPE[7]. Mice homozygous for a hypomorphic mutation in *Zic2* (*Zic2*$^{kd/kd}$) show embryonic or perinatal lethality with HPE-like symptoms and other anomalies[8–11], suggesting that the role of *Zic2* in forebrain development is largely conserved between human and mouse.

The role of Zic2 in embryonic development has been well-studied, but its role in the mature brain and/or the consequences of developmental Zic2 insufficiency in mature animals has not been fully investigated. It is possible that hypomorphic mutations that do not cause embryonic/perinatal lethality have a profound influence on higher brain functions. A pilot investigation analyzing the behavior of mice heterozygous for the hypomorphic mutation in *Zic2* (*Zic2*$^{kd/+}$) showed some abnormalities of the acoustic startle response[12]. However, the behaviors examined in that study were limited. A more comprehensive analysis is needed to clarify the causal relationship between the hypomorphic in *Zic2* and behavioral abnormalities that might underlie neuropsychiatric disorders such as schizophrenia.

Schizophrenia is a relatively common mental disorder that affects 1% of the population worldwide. The disease is characterized by positive symptoms (delusions and hallucinations), negative symptoms (affective flattening and social withdrawal), and cognitive dysfunction (deficits in working memory, attention, processing speed, and executive function)[13,14]. Morphologically, there are abnormalities of the brain that are frequently found in schizophrenia, such as enlarged ventricles, dendritic changes in the pyramidal neurons, and alteration of specific subtypes of interneurons[15–18]. Although the molecular basis of the disease is not fully understood, rare gene mutations that exert large effects in the susceptibility of schizophrenia, in addition to multiple common single nucleotide polymorphisms (SNPs), are being accumulated[19–22].

Here, we first performed comprehensive analyses of the *Zic2*$^{kd/+}$ mice in manifold behavioral test situations and by morphological and histological examinations. Then, since the results suggested that the *Zic2*$^{kd/+}$ mice mimic the schizophrenia-like phenotypes, we undertook resequencing analysis of the *ZIC2* gene using DNA isolated from patients with schizophrenia and from controls. One mutation, R409P, was shown to have impaired transcription activity, DNA-binding ability, and cofactor-binding capacity. These results were discussed in terms of the pathogenesis of schizophrenia.

Results

Wild-type (*Zic2*$^{+/+}$) and *Zic2*$^{kd/+}$ mice are indistinguishable by their body weight and external appearance[12]. Both male and female *Zic2*$^{kd/+}$ mice are fertile and female *Zic2*$^{kd/+}$ mice can foster their progenies without any obvious faults[8]. In our previous study, we found that prepulse inhibition (PPI) of acoustic startle response is decreased in *Zic2*$^{kd/+}$ mice[12]. For a more comprehensive analysis of behavioral phenotypes, we carried out the suite of behavioral tests listed in Table 1. For the light-dark box test, marble burying test, elevated plus maze test, forced swimming test, grip strength test, wire hanging test, footprint test and rotarod test, we found no significant differences in behavior between *Zic2*$^{kd/+}$ and wild-type mice (Table 1)[12]. For the remaining tests, we found significant differences in behavior between *Zic2*$^{kd/+}$ and wild-type mice; as described below.

Locomotor activities were lower or higher in *Zic2*$^{kd/+}$ mice than wild-type mice depending on the situation. We first placed the mice in new home cages and then monitored their locomotor activity continuously for 13 days (Figure 1A–C). Our analysis revealed that the locomotor activity was significantly lower in *Zic2*$^{kd/+}$ mice than in wild-type mice in the later stationary period (relatively low day-to-day variance, days 6–13) ($P = 0.044$) (Figure 1A). When we assessed the mean circadian locomotor activities during the stationary period, we found that the activity of *Zic2*$^{kd/+}$ mice was significantly lower than that of the wild type in the early dark phase (20:00–24:00) ($P = 0.048$), but that the circadian rhythm of the *Zic2*$^{kd/+}$ mice was normal (Figure 1B).

We also assessed locomotor activity in open field tests with observation times of 15 min. *Zic2*$^{kd/+}$ mice showed a significantly higher overall locomotor activity compared to wild-type mice ($P = 0.041$) (Figure 1C, left), but there were no differences in preference between the two genotypes for the central and peripheral fields (Figure 1C, right). These results suggest that *Zic2*$^{kd/+}$ mice have higher locomotor activities than the wild type in a novel environment.

Cognitive function deficits in *Zic2*$^{kd/+}$ mice. The Morris water maze test is commonly used to evaluate learning ability and acquisition of spatial memory. In our study, this test consisted of 4 days of training (day 1–4) with a fixed hidden platform, 1 day (day 5) of a probe test without a platform, and 1 day (day 6) of a reverse test in which the hidden platform was placed in the opposite quadrant. To reach the hidden platform, *Zic2*$^{kd/+}$ mice needed a significantly longer time in the training session ($P = 0.046$) and a significantly longer time in the reverse test session ($P = 0.037$) (Figure 2A, top panel). The moving speed of *Zic2*$^{kd/+}$ mice was slightly, and significantly, lower than that of wild-type mice only on day 1 of the training session (Figure 2A, left middle panel, $P = 0.036$). However, their spatial memory acquisition was not impaired as seen in the results of the probe test (Figure 2A, bottom panel). The motor performance and motivation of *Zic2*$^{kd/+}$ mice might not be impaired, given that there were no significant differences between the two genotypes in the moving speed at days 2 to 4 [$F(1,18) = 0.017$, $P = 0.90$, RMANOVA, main effect of genotype] (Figure 2A, left middle panel) or in the overall no movement time [$F(1,18) = 0.23$, $P = 0.64$, RMANOVA, main effect of genotype] (Figure 2A, right middle panel). Further supporting this notion, the results were similar for *Zic2*$^{kd/+}$ and wild-type mice for the other tests related to motor performance and motivation (rotarod, footprint, wire hanging and forced swimming test) (Table 1). Therefore, the water maze test results were considered to reflect an impaired learning ability of *Zic2*$^{kd/+}$ mice.

Fear conditioning is a test for associative learning that depends partly on hippocampal function, as is the Morris water maze test. The association of conditioned stimuli (CS, tone) and unconditioned noxious stimuli (US, electric foot shock) was learned in the conditioning on day 1. The results were quantitatively evaluated by the freezing response of the subjects. *Zic2*$^{kd/+}$ mice showed a significantly reduced freezing response in the context test on day 2 ($P = 0.037$, U-test, Figure 2B). These mice also showed a significantly reduced freezing response in the cue test on day 3 ($P = 0.049$, U-test, Figure 2C).

We also observed abnormal behavioral traits in *Zic2*$^{kd/+}$ mice in the Y-maze spontaneous alternation test. *Zic2*$^{kd/+}$ mice showed a significantly lower alteration percentage ($P = 0.046$, U-test) and a significantly higher number of arm entries ($P = 0.0040$) than the wild-type mice (Figure 2C), suggesting that *Zic2*$^{kd/+}$ mice have working memory impairment and a higher level of locomotor activity in a novel environment. Together with the absence of behavioral traits related to mood disturbances or anxiety-like behaviors, our results from the water maze, fear-conditioning and Y-maze tests are consistent with the impaired cognitive function in *Zic2*$^{kd/+}$mice.

Abnormalities in social behavior in *Zic2*$^{kd/+}$ mice. We next assessed the social behaviors of the *Zic2*$^{kd/+}$ mice by the resident-intruder assay. Juvenile wild-type mice were placed into the home cages of

Table 1 | Summary of *Zic2*$^{kd/+}$ behavioral analysis.

Test	Response[1]	Implication to schizophrenia[2]
Home cage activity	decreased*	Negative?
Open field		
Locomotor	increased*	Positive (psychomotor agitation)
% center	no change	
Morris Water Maze		
Latency-training	increased*	
Latency-reverse	increased*	Cognitive (learning deficits)
Probe test	no change	
Speed-training	initially slow*	
No move-training	no change	
Fear conditioning		
Conditioning	no change	
Contextual	decreased*	Cognitive (fear memory deficits)
Cue	slightly decreased*	
Y-maze		
No. of entries	increased*	Positive (psychomotor agitation)
% alteration	decreased*	Cognitive (working memory deficits)
Social interaction		
Novel environment	no change	
Resident intruder	attack decreased*	Negative (social withdrawal)
Social dominance	often loser*	Negative (social withdrawal)
Social recognition	no change	
Acoustic startle response	increased*[3]	Cognitive (sensorimotor gating)
PPI of acoustic startle response	decreased*[3]	Cognitive (sensorimotor gating)
Light-Dark box	no change	
Marble burying	no change	
Burrowing	no change	
Elevated Plus maze	no change[3]	
Forced swimming	no change[3]	
Tail suspension	no change	
Grip strength	no change[3]	
Wire hanging	no change[3]	
Footprint	no change[3]	
Rotarod	no change[3]	

[1] *Zic2*$^{kd/+}$ compared to *Zic2*$^{+/+}$; [2] Possible relevance to the three classes of schizophrenia symptoms (positive, negative, and cognitive dysfunction); [3] Ogura et al. (2001) [12]; *$P < 0.05$ in statistical tests between *Zic2*$^{+/+}$ and *Zic2*$^{kd/+}$.

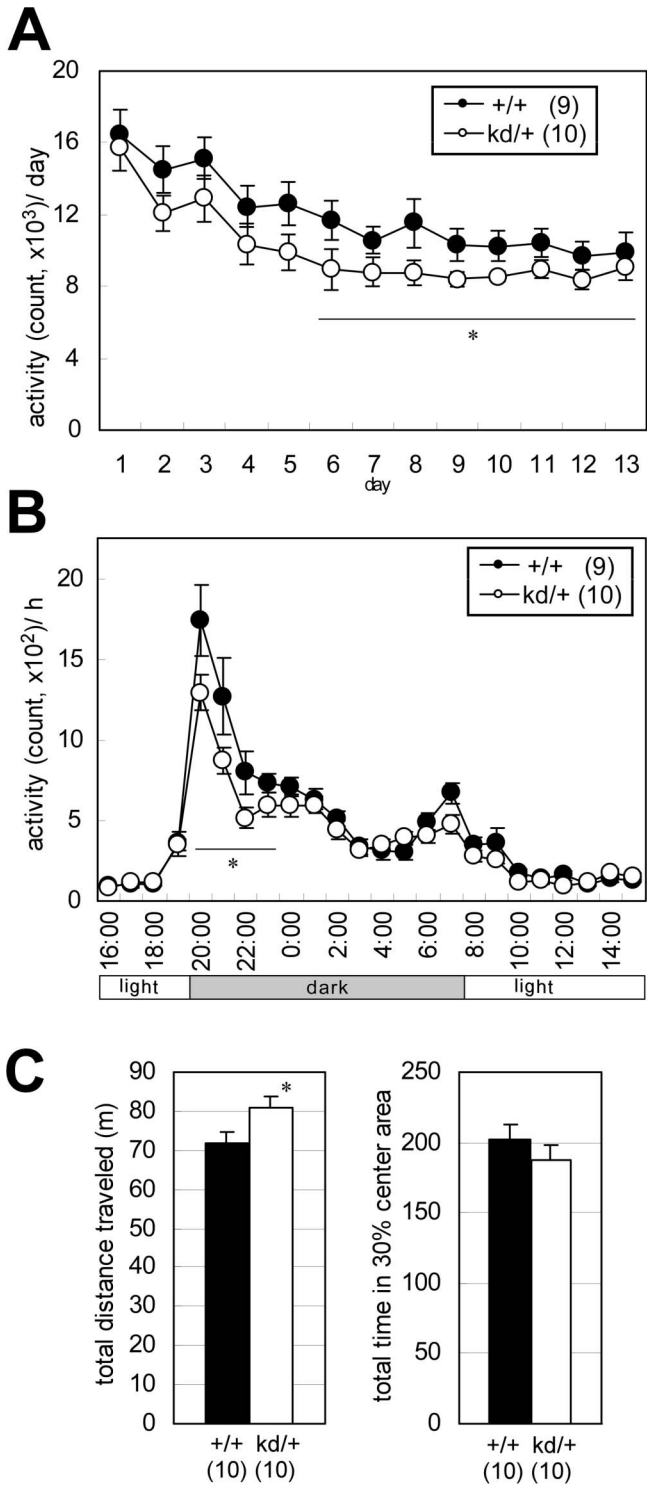

Figure 1 | Spontaneous motor performance abnormalities in *Zic2*$^{kd/+}$ mice. (A) Home cage activity was measured for 13 days. On day 1 the mice were put into a new home cage. Mean activities per day are indicated. Activity counts represent the number of time bins (approximately 0.20–0.25 s each) in which spontaneous activity including locomotor activity, rearing, and other activities such as stereotypic movements, were detected. *$P < 0.05$ in t-test. (B) Circadian activities. The values indicate the summation of the activities corresponding time bins (bin= 1 h) of the last 8 days (days 6–13) when the daily change in the total activity level (A) was minimal. *$P < 0.05$ in t-test. (C) Open field test. (left) Total distance traveled in the open box for 15 min observation period. (right) Percentage of the total time in the central area of the field (30% of the total field area). *$P < 0.05$ in t-test. Data is presented as means ± SEM. The number of mice in each group is given in parentheses.

the resident *Zic2*$^{kd/+}$ mice and the behavior of the test mice (*Zic2*$^{kd/+}$ mice or control wild-type mice) were analyzed for 15 min (Figure 3A, 3B, supplemental video). The time spent attacking ($P = 0.049$; Figure 3A, left panel) and the frequency of attacks were significantly lower in *Zic2*$^{kd/+}$ mice than in control wild-type mice ($P = 0.049$; Figure 3A, right panel). The frequency of body contact also tended to be higher in *Zic2*$^{kd/+}$ mice than in wild-type mice ($P = 0.12$). We also observed abnormal social behavior in *Zic2*$^{kd/+}$ mice in the social dominance tube test (Figure 3C). In this test, *Zic2*$^{kd/+}$ mice and control wild-type mice were placed at opposite ends of a transparent plastic tube in a head-to-head direction, and the first mouse to escape was judged the loser (Figure 3B). In general, mice of both genotypes moved forward and pushed each other within the tube. *Zic2*$^{kd/+}$ mice became losers more frequently than the wild-type mice ($P = 0.024$, chi-square test). We also performed a social interaction test in a novel environment (open field) with caged (Figure S1B) and non-caged partners (Figure S1A), but found no clear differences in the number and duration of the contacts between *Zic2*$^{kd/+}$ and wild-type mice.

***Zic2*$^{kd/+}$ mouse brain shows an altered morphology and reduction of forebrain cholinergic neurons and amygdalar Zic-positive cells.** To elucidate the molecular basis of the behavioral abnormalities observed in *Zic2*$^{kd/+}$ mice, we performed a morphometric analysis of the *Zic2*$^{kd/+}$ mouse brain by MRI (Figure 4). We showed that *Zic2*$^{kd/+}$ mouse brains had enlarged lateral ventricles compared with the brains of wild-type mice (Figure 4A and B). The ratio of the volume of lateral ventricles to brain was 35% higher in the brains of *Zic2*$^{kd/+}$ mice than in those of wild-type mice. The 3D superimposition of lateral ventricles in the brain indicated that the enlargement was most notable in the anterior horn region (Figure 4B and C). Enlargement of the lateral ventricles in *Zic2*$^{kd/+}$ mice might partly reflect the reduction in the mass of the septum (Figure 4A, right panel), which we also observed in MRI 2D coronal images through the anterior commissure (data not shown). The hippocampal size did not show any clear differences between the two genotypes. Morphometric analysis of histological sections revealed that compared to the wild type the thickness of the cerebral cortex and the corpus callosum was slightly but significantly thinner in *Zic2*$^{kd/+}$ mice (cerebral cortex, $P = 0.0038$; corpus callosum, $P = 0.0028$; Figure 4D) and that the position and shape of the medial structure rostral to the hippocampus (fimbria including septofimbrial nucleus or septal triangular nucleus) were significantly narrower ($P < 0.001$ for both, Figure 4D).

We also found the amygdala in *Zic2*$^{kd/+}$ mice to be morphologically different to that in wild-type mice. In wild-type mice, Zic-positive cells were abundant in the amygdalohippocampal area (AHA) and sparse in the medial and cortical nuclei (Figure 4E). In *Zic2*$^{kd/+}$mice, the Zic-positive cells were less abundant than in wild-type mice in the equivalent rostrocaudal positions (Figure 4E, 8/8). Furthermore, the high cell density in the AHA of wild type animals shown in toluidine blue staining seemed reduced and the intense signals detected by acetylcholine esterase staining in the AHA was debilitated (Figure 4E), in *Zic2*$^{kd/+}$ mice. As shown by acetylcholine esterase stained sections (Figure 4E), in some cases (6/8), the medial protrusion of the amygdala in the coronal sections tended to be blunted in *Zic2*$^{kd/+}$ mice compared to the wild type.

The reduction of the septal mass and expression of *Zic2* in the basal forebrain structures[10] led us to investigate the number of cholinergic neurons that are densely distributed in the septum. We counted the choline acetyl transferase (ChAT)-positive cholinergic neurons in comparable coronal sections from the brains of *Zic2*$^{kd/+}$ and wild-type mice. The results indicated that the numbers of cholinergic neurons were decreased in the medial septum, diagonal band and substantia innominata regions, but not in other regions including cerebral cortex, striatum and caudoputamen, (Figure 5A–C). In

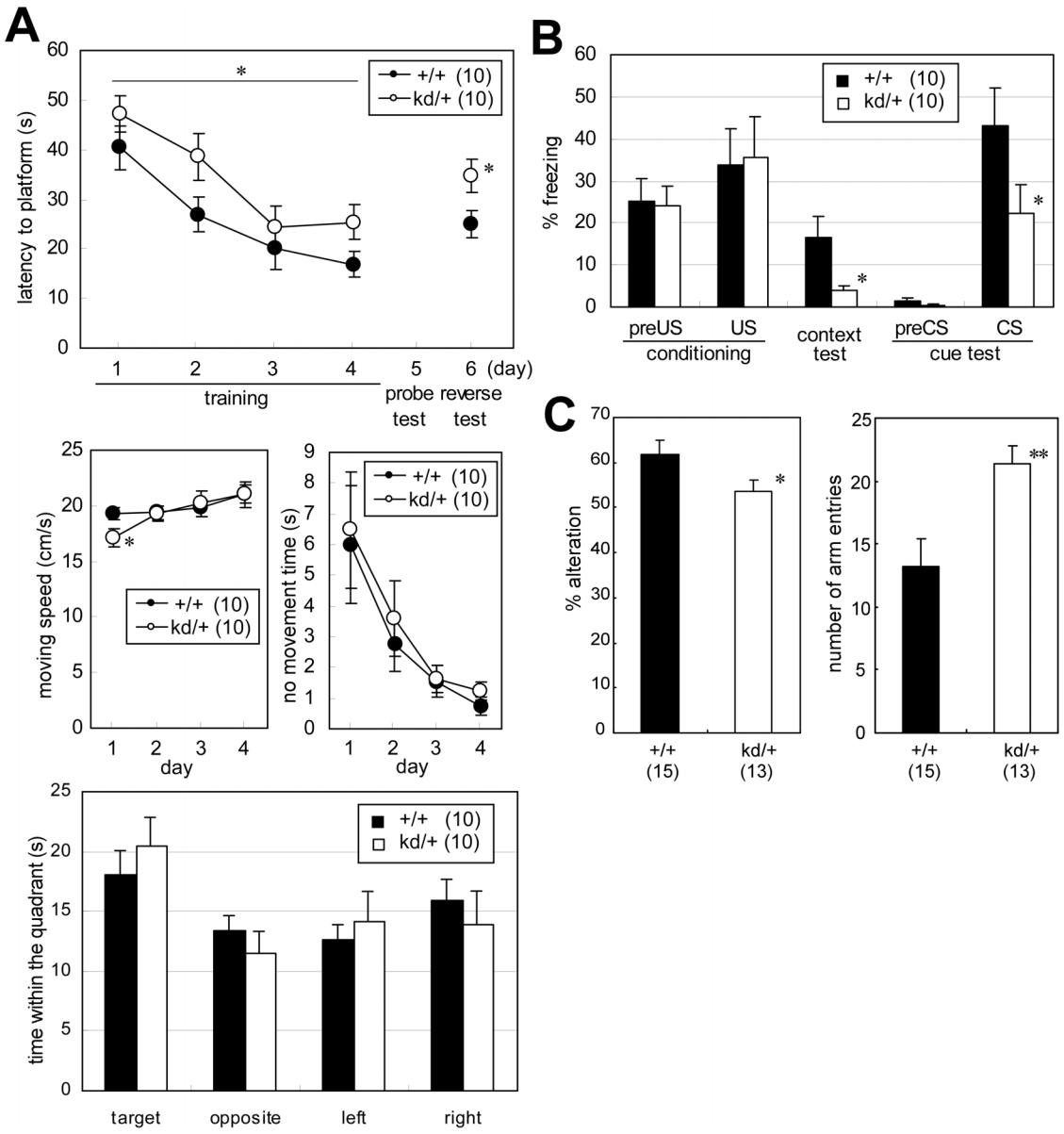

Figure 2 | Cognitive function deficits in *Zic2*$^{kd/+}$ mice. (A) Morris water maze test. (top) Mean latency to reach the platform during the training session (days 1–4) and reverse test session (day 6). Values indicate the mean of all six trials on the day. (middle left) Moving speed in the training session. (middle right) No movement time in the training session. (bottom) The results of the probe test (day 5) as indicated by the period of time (s) in the indicated quadrant within the 60 s testing period. *$P < 0.05$ in t-test. (B) Fear conditioning test. Mean percentage freezing are indicated for the conditioning test (day 1) before and after the electrical foot shock (preUS [mean of the 2 min before unconditioned-stimulus, US] and US [1 min after US] respectively), context test (day 2, mean of the total testing period [5 min]), and cue test (day 3) before and after pre tone (preCS [mean of the 2 min before conditioned stimulus, CS] and CS [mean of the 2 min with CS], respectively). *$P < 0.05$ in Mann-Whitney U-test. (C) Y-maze test. (left) Percentage altered selection of the entered arm. (right) Total number of arm entries. *$P < 0.05$ in Mann-Whitney U-test; **$P < 0.01$ in t-test. Data is presented as means ± SEM. The number of mice in each group is given in parentheses.

addition, the numbers of PV-positive neurons were not different in the medial septum or diagnonal band (Figure 5D). Therefore, the number of basal forebrain cholinergic neurons is selectively reduced by the reduction of *Zic2* expression. We also examined the number of ChAT-positive cells with or without Zic-like immunoreactivities in the affected regions (medial septum, diagonal band and substantia innominata) at early postnatal stages (P5–7, Figure 5E). In *Zic2*$^{kd/+}$ mice, we observed a significant reduction in the number of Zic$^-$ChAT$^+$ cells in the diagonal band region compared to the number in wild-type mice ($P < 0.001$, Figure 5E, left panel). The number of Zic$^-$ChAT$^+$ cells in the medial septum and Zic$^+$ChAT$^+$ cells in the diagonal band and medial septum region also tended to be reduced in *Zic2*$^{kd/+}$ mice compared to the wild type (Zic$^-$ChAT$^+$ cells in the medial septum, $P = 0.062$; Zic$^+$ChAT$^+$ cells in the diagonal band and medial septum region, $P = 0.12$ and $P = 0.056$ respectively). These results were consistent with those obtained in adult mice, suggesting that the reduction in the number of ChAT-positive neurons in the basal forebrain primarily stemmed from the reduction in *Zic2* gene expression during embryonic or prenatal development. In addition, we found that the number of Zic$^+$ChAT$^-$ cells was significantly increased in the diagonal band region and medial septum in *Zic2*$^{kd/+}$ mice compared to wild-type mice (diagonal band, $P = 0.039$; medial septum, $P = 0.047$ respectively; Figure 5E, right panel).

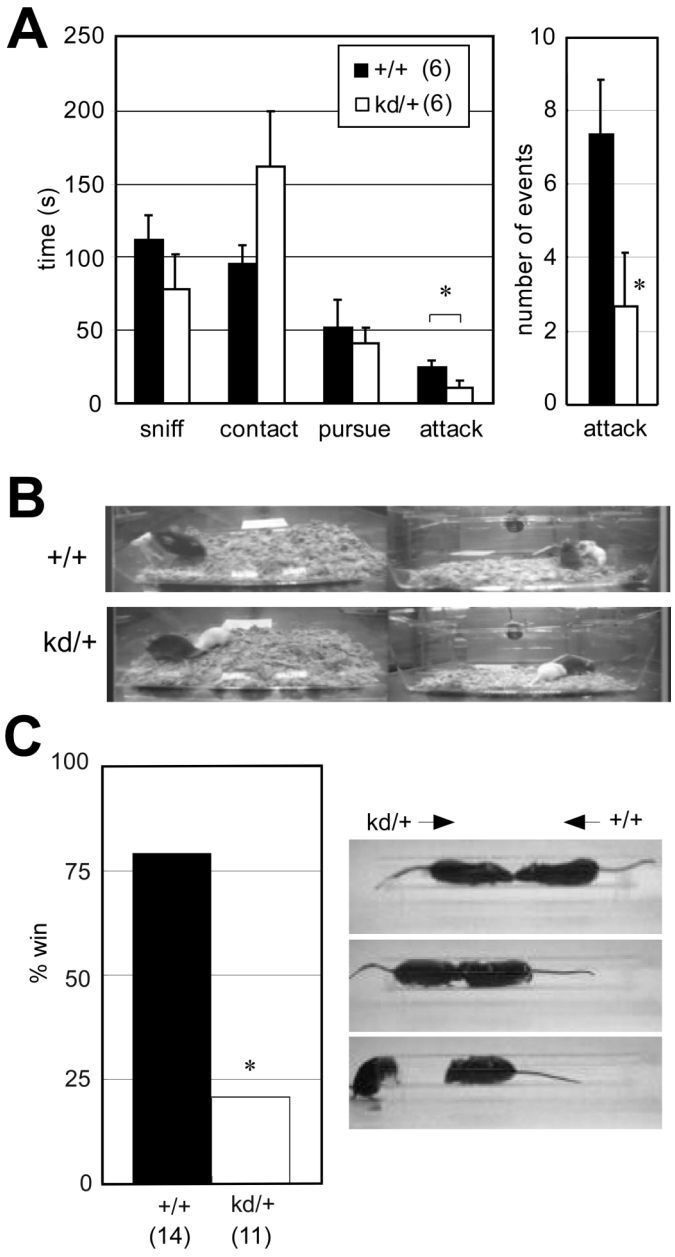

Figure 3 | Social behavior abnormalities in *Zic2*$^{kd/+}$ mice. (A) Resident-intruder test. (left) Total time spent in the indicated behaviors. (right) The number of attacking events. *$P < 0.05$ in t-test. Data is presented as means ± SEM. (B) Captured video image of the resident-intruder test. In this case, the *Zic2*$^{+/+}$ mouse (+/+, top, black) was attacking the white intruder mouse, whereas the *Zic2*$^{kd/+}$ mouse (kd/+, bottom black) was moving away from the intruder mouse. The left and right images indicate the simultaneous recording from opposite directions. (C) Social dominance tube test. (left) Won rate in the total of 66 matches. The means ± SEM latencies to win were as follows: *Zic2*$^{+/+}$, 36.5 ± 5.2; *Zic2*$^{kd/+}$, 38.3 ± 6.4 s. (right) Captured video images from a representative match. From top to bottom, the beginning to the end of the match is sequentially indicated. In this case, the *Zic2*$^{kd/+}$ mouse was pushed out from the plexiglass tube (30 cm) and the *Zic2*$^{+/+}$ mouse became the winner. *$P < 0.05$ in chi-square test. The number of mice in each group is given in parentheses.

Screening of *ZIC2* mutations in patients with schizophrenia. Some of the above behavioral and histological abnormalities in *Zic2*$^{kd/+}$mice are reminiscent of schizophrenia symptoms in humans. We therefore set out to examine whether *ZIC2* mutations contribute to the onset of schizophrenia, in at least a subset of patients. As a first step to address this possibility, we searched *ZIC2* for nonsynonymous mutations in patients with schizophrenia. Many nonsynonymous mutations are reported in patients with HPE[6,23]; however, there are no reports of an association of *ZIC2* mutations with psychiatric illnesses.

Sequence analysis of the entire *ZIC2* protein coding regions and adjacent introns in 278 patients revealed four nonsynonymous mutations in the coding regions (Table 2). We then examined the allele frequencies of these mutations in 967 patients with schizophrenia and in 1060 control subjects (Table 2). Ins239H was the most commonly detected mutation, but its frequency (~9%) was similar in patient and control groups. This finding is consistent with the results of previous studies[7,24–27]. The three remaining mutations, A95T, R409P, and S444R, were novel. A95T and R409P were singleton mutations not found in normal subjects. The frequency of S444R was not significantly different between the patient group (0.39%) and normal subjects (0.18%; $P = 0.80$ by Fisher's exact test). Patients with this mutation showed no obvious psychotic symptoms; however, we could not perform detailed physical examinations on these patients, nor examine the genotypes of their relatives because we could not obtain their consent on these issues.

The *Zic2*-R409P shows impaired transcriptional activation. Zic orthologues are widely distributed among the eumetazoans and show evolutionary conserved domains in their protein-coding regions[28]. Multi-species alignment of the three *Zic2* mutations revealed that R409P was located within the highly conserved regions of the published Zic sequences, including those of the protostomians and cnidarians (Figure 6A and data not shown). We also showed that R409 position has conserved in a zinc-finger-type transcription factor, GLI1, in which the side chain of the encoded amino acid residue is responsible for side-chain-base interactions (Figure S2)[29]. Both A95T and S444R were conserved in most of the vertebrate *Zic2* sequences examined, but these sequences did not align with those in invertebrates (Figure 6A and data not shown). We used the computer algorithm PolyPhen Polyphen[30] to predict the effect of the mutations on protein structure and function. PolyPhen analysis predicted that the amino acid change in R409P most likely caused abnormal protein structure and function, whereas it was only a possibility for S444R and even less likely for A95T (Table 2).

We characterized the function of these mutations by generating the equivalent mutations in mouse Zic2 proteins, and assessing their activities in vitro. The size of the mutant Zic2 proteins was mostly comparable to that of the wild type protein, as shown by sodium dodecyl sulfate-polyacrylamide gel electrophoresis (SDS-PAGE) analysis (Figure 6B). However, the band corresponding to Zic2-S444R also contained a fast migrating component in preparations from both transfected mammalian cells and from in vitro translation (Figure 6B and data not shown). The nuclear localization capacity of the mutant proteins was significantly reduced for R409P ($P < 0.001$ in chi-square test), but not for A95T or S444R (Figure S2). Zic2 can be a transcriptional activator[31,32]. We assessed the transactivating activity of the mutant proteins by co-transfecting mammalian cells with expression vectors that express the proteins. The Zic2-R409P protein, but not the Zic2-A95T or Zic2-S444R proteins had significantly reduced transactivating capacity compared to the wild-type protein ($P < 0.001$, Figure 6C); the normalized activation capacity of Zic2-R409P was approximately 20% that of the wild-type protein. When we examined the effect of the R409P mutation on the capacity to bind a high-affinity Zic-binding sequence, Zic2-R409P showed lower binding affinity to the target sequences than wild-type Zic2 (Figure 6D and 6E). Zic2 is known to complex with the DNA-PK catalytic subunit and RHA[33]. As shown in immunoprecipitation experiments (Figure 6F), the binding affinity of Zic2-R409P to DNA-PK, but not to RHA, was reduced compared to wild-type

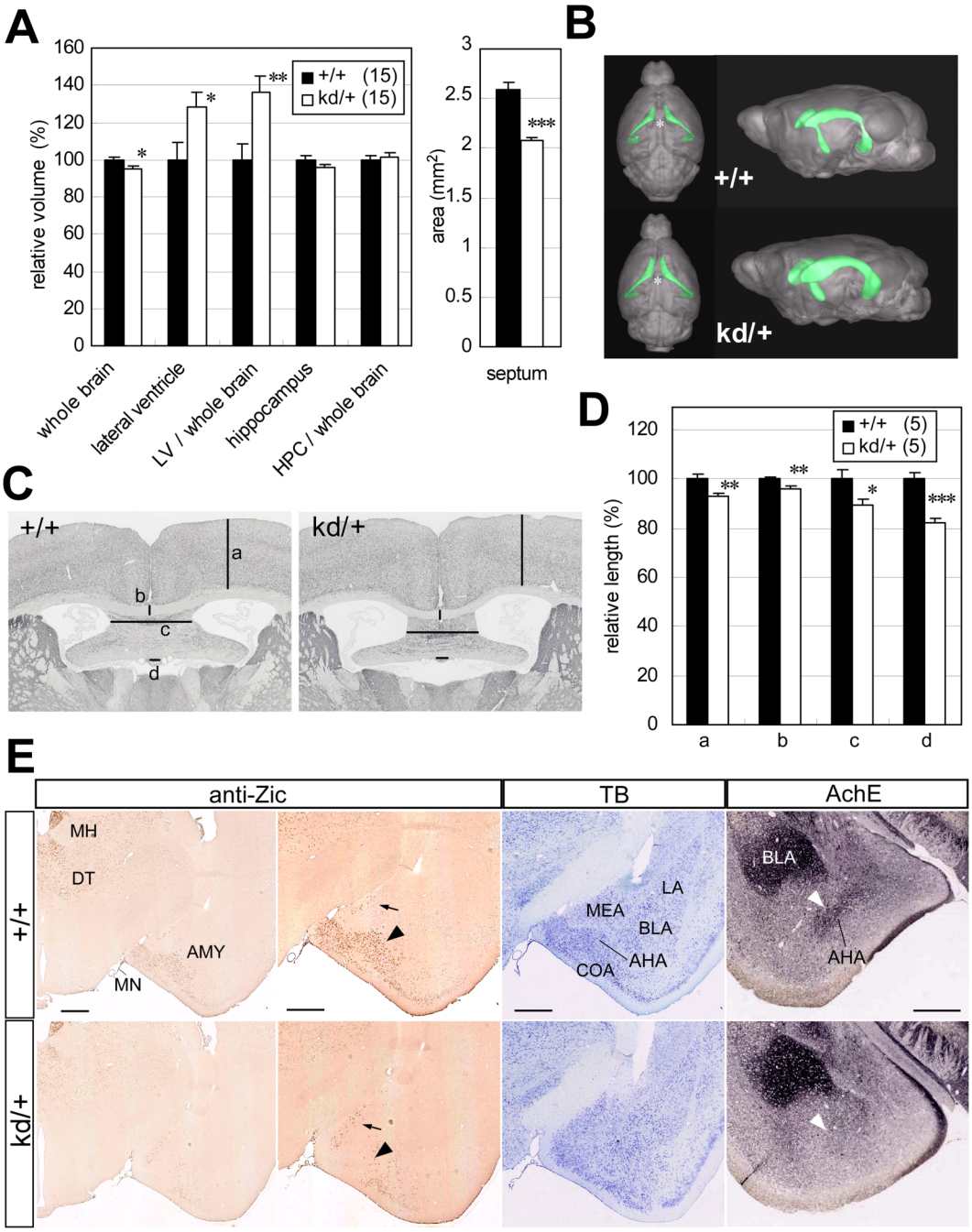

Figure 4 | Morphological features of the brains from *Zic2*$^{kd/+}$ mice. (A) Volumetric analysis of the entire brain, lateral ventricle (LV), and hippocampus (HPC). The values for tissue volumes in *Zic2*$^{kd/+}$ mice are indicated as percentages of the corresponding wild-type values. The values for ratio of volumes in LV/whole brain and HPC/whole brain are also indicated as percentages of the corresponding wild-type values. A total of 15 pairs of *Zic2*$^{+/+}$ and *Zic2*$^{kd/+}$ mice were subjected to in vivo MRI imaging. $*P < 0.05$, $**P < 0.01$, $***P < 0.001$ in t-test. Data is presented as means ± SEM. (B) 3D reconstruction of the outer surface of the brains of *Zic2*$^{+/+}$ (+/+) and *Zic2*$^{kd/+}$ (kd/+) mice (gray) with lateral ventricle (green). Dorsal (left) and anterior-lateral (right) views are indicated. Note the enlarged lateral ventricles and the narrowed interspace between the left and right lateral ventricles containing septum (asterisk). (C) Morphometric analysis. Sections were subjected to acetylcholine esterase staining. (a)–(d) Lines denote the distances measured in each section (a, cerebral cortex thickness; b, corpus callosum thickness; c, medial structure rostral to the hippocampus [fimbria including septofimbrial nucleus or septal triangular nucleus]; d, subfornical organ width). The measurements were done on 15 pairs of the most comparable from the serial sections of adult male *Zic2*$^{+/+}$ and *Zic2*$^{kd/+}$ mice brains. (D) Morphometric analysis. The lengths are presented as a percentage relative to the corresponding wild-type values. $*P < 0.05$, $**P < 0.01$, $***P < 0.001$ in t-test. Data is presented as means ± SEM. (E) Morphological abnormalities in the amygdala. The coronal sections from *Zic2*$^{+/+}$ (+/+) and *Zic2*$^{kd/+}$ (kd/+) mice were subjected to immunostaining with the anti-Zic antibody, toluidine blue (TB), and acetylcholine esterase staining (AchE). The black arrowhead and arrow indicate the Zic-positive cells in the amygdalohippocampal area (AHA) and medial nucleus, respectively. The white arrowheads indicate the enhanced AchE signals in the AHA. AMY, amygdalar complex; BLA, basolateral nucleus of amygdala; COA, cortical nucleus of amygdala; DT, dorsal thalamic nuclei; LA, lateral nucleus of amygdala; MEA, medial nucleus of amygdala; MH, medial habenular nucleus; MN, meningeal membrane. Scale bars, 0.5 mm.

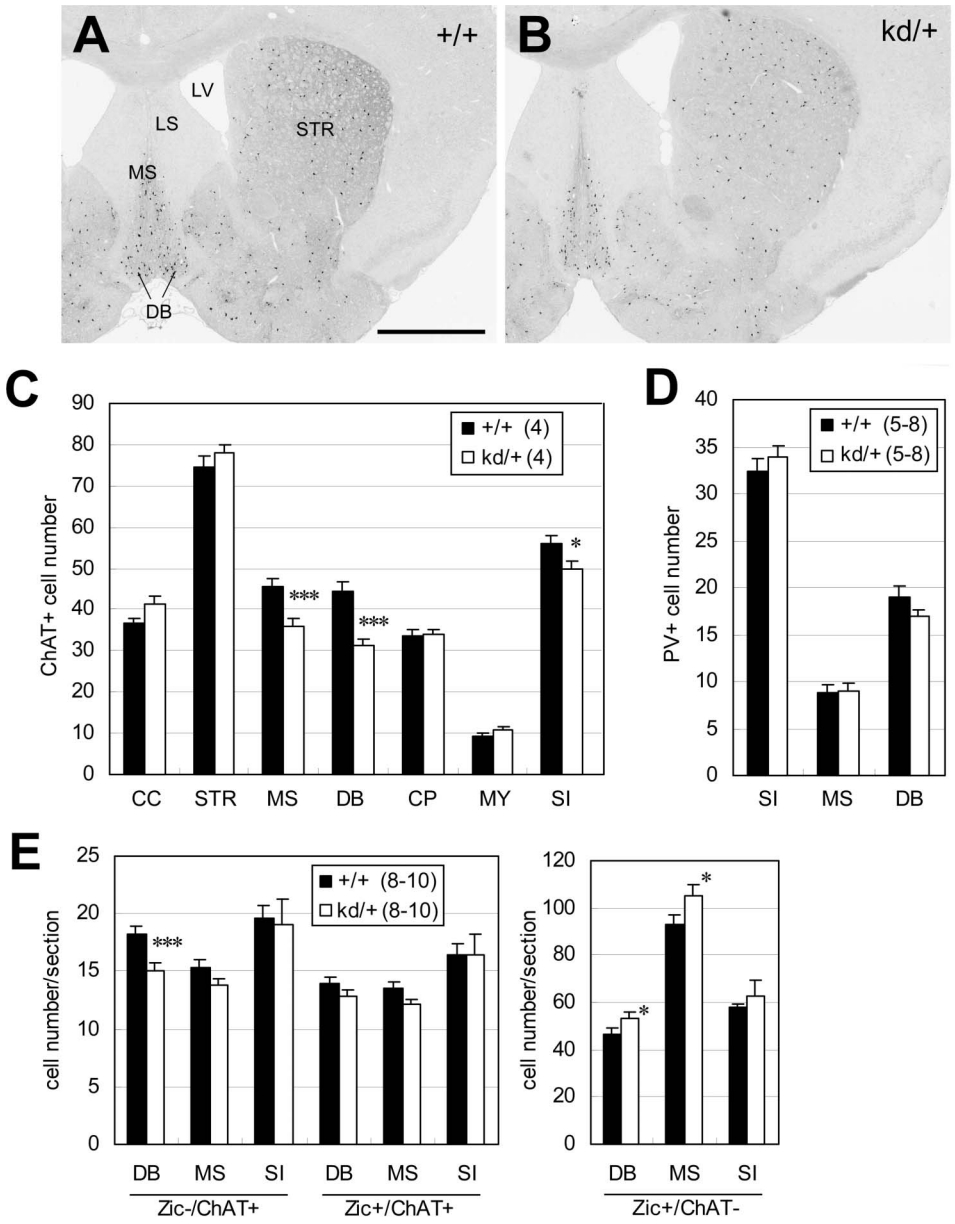

Figure 5 | Decreased number of cholinergic neurons in the brains of *Zic2*$^{kd/+}$ mice. (A,B) Immunostaining of the brains of *Zic2*$^{+/+}$ (+/+) (A) and *Zic2*$^{kd/+}$ (kd/+) (B) mice with anti-ChAT antibody. Coronal sections through the septum and diagonal bands derived from adult male mice were subjected to immunoperoxidase staining. Scale bar, 1 mm. (C) Number of the ChAT^{+} neurons in the sections. Mean numbers of ChAT^{+} neurons in 20 sections from the *Zic2*$^{+/+}$ and *Zic2*$^{kd/+}$ mice brains are indicated. (D) PV-positive cell numbers. The measurements were taken in comparable regions to those subjected to ChAT-immunostaining. (E) The numbers of ChAT- and Zic-immunoreactive neurons in early postnatal (P5-7) *Zic2*$^{+/+}$ and *Zic2*$^{kd/+}$ brains. Double labeling was performed with the anti-ChAT antibody and anti-pan Zic antibody. CC, cerebral cortex; CP, caudoputamen; DB, diagonal band; LV, lateral ventricle; LS, lateral septum; MS, medial septum; MY, Mynert nucleus; SI, substantia innominata; STR, striatum. (C–E) Data is presented as means ± SEM. The number of mice in each group is given in parentheses. *$P < 0.05$, ***$P < 0.001$ in t-test.

Zic2. Taken together, these results suggested that the R409P mutation dampens the transcriptional activation capacity of Zic2 by altering the properties of the Zic2-containing molecular complex.

Discussion

Our behavioral analysis in mice uncovered some novel roles of Zic2 related to higher brain function. A summary of the results from this behavioral analysis and that of previous studies is provided in Table 1.

The locomotor activity differences between wild-type and *Zic2*$^{kd/+}$ mice were context-dependent. In home cages, the mutant mice showed reduced locomotor activity in the early dark phase compared to wild-type mice, but in the open field test the mutant mice showed higher locomotor activity than wild-type mice. The tendency for *Zic2*$^{kd/+}$ mice to display higher activity in a novel environment, compared to wild-type mice was also observed in the the Y-maze test and the light-dark box test (Figure S1C). Therefore, *Zic2*$^{kd/+}$ mice appear to be generally hyperactive upon exposure to a novel environment. This hyperactivity is possibly consistent with symptoms of schizophrenia in humans; hyperactivity in response to a novel environment has been suggested as a useful animal correlate of schizophrenia symptoms[34] and has been noted in some genetically engineered mouse models of schizophrenia[35–37].

We demonstrated cognitive dysfunction in *Zic2*$^{kd/+}$ mice by the water maze test, the fear-conditioning test, and the Y-maze test. In addition, abnormal PPI, which is deemed to reflect impaired

Table 2 | Allelic frequencies of non-synonymous mutations in the *ZIC2* gene in patients with schizophrenia and control subjects.

	Control				Schizophrenia				
Polymorphism	Genotype count			MAF[2]	Genotype count			MAF	Polyphen (PSIC)[1]
Ala95Thr (283G>A)	G/G	G/A	A/A	0	G/G	G/A	A/A	0.041	Benign (0.897)
	1,036	0	0		1,226	1	0		
Ins239His	del/del	del/ins	ins/ins	8.95	del/del	del/ins	ins/ins	8.77	
	865	173	7		1,025	198	9		
Arg409Pro	G/G	G/C	C/C	0	G/G	G/C	C/C	0.04	Probably damaging (2.745)
(1,226G>C)	1,058	0	0		1,238	1	0		
Ser444Arg	C/C	C/A	A/A	0.284	C/C	C/A	A/A	0.363	Possibly damaging (1.541)
(1,332C>A)	1,051	6	0		1,230	9	0		

[1]Polyphen is a computer algorithm used to predict the effects of non-synonymous single-nucleotide polymorphisms (SNPs) on protein structure and function [30]. PSIC, difference in position-specific independent counts.
[2]MAF, minor allele frequency

sensorimoter-gating function seen in schizophrenia, is reported in *Zic2*$^{kd/+}$ [12]. These results corroborate that the cognitive function deficits in *Zic2*$^{kd/+}$ mice are not simple, but multimodal ones including sensorimotor gating function.

Social behavioral abnormalities in *Zic2*$^{kd/+}$ mice were characterized by a reduction in aggressive behavior compared to the wild-type controls in the absence of clear deficits in the affiliative behaviors. The aggressivity assessed in the resident-intruder and social dominance tube tests may be related to their territory protecting behavior. The absence of depression-like behavior in these mice excludes the possibility that their reduced aggressivity was the result of a general loss in motivation.

Collectively, the behavioral phenotypes of *Zic2*$^{kd/+}$ mice seem to be implicated in the three classes of schizophrenia symptoms (positive/negative symptoms and cognitive dysfunction). When we compare the *Zic2*$^{kd/+}$ mice phenotype with those of other typical schizophrenia model mice (Table 3), novelty-induced hyperactivity and prepulse inhibition reduction were commonly found in the dominant negative DISC1 transgenic[38]and NRG1 transmembrane KO[35]and conditional KO of ErbB4 in PV-positive interneuron[39]. In addition, the enlargement of lateral ventricle and decrement of working memory were shared with *Zic2*$^{kd/+}$ and some of them (Table 3).

The morphological abnormalities in the brain of *Zic2*$^{kd/}$ include a reduction in the septal mass, thinning of the cerebral cortex and corpus callosum, narrowing of the fimbria hippocampi, and a regional reduction of amygdalar nuclei. These abnormalities have a pathophysiological resemblance to neuropsychiatric disorders in humans. In particular, enlarged lateral ventricles and decrease in whole brain volume are a symptom of the first episode of schizophrenia[16–18], and have been observed in some genetically-engineered mouse models of schizophrenia[15,37,38,40,41]. These finding add further support for the genetic involvement of *ZIC2* in the pathogenesis of schizophrenia.

Regarding the basis of neural circuits underlying the higher brain function abnormalities observed in *Zic2*$^{kd/+}$mice, we consider the following two observations to be significant. Firstly, we observed a reduction in the number of cholinergic neurons in the basal forebrain, which raises the possibility that abnormal cholinergic regulation of higher brain function underlies the behavioral abnormalities seen in *Zic2*$^{kd/+}$ mice. Basal forebrain cholinergic neurons are thought to be capable of regulating the cortical processing of sensory stimuli within various domains[42]. In addition, recent studies indicate that the cholinergic system modulates cognitive deficits in schizophrenia and that cholinergic transmission is a potential target of therapeutics for the improvement of cognitive functions[43]. Thus, further evaluation of the cholinergic transmission dynamics in *Zic2* mutants would be beneficial for a better understanding of the role of Zic2 in cognitive function. We also examined the distribution of PV-positive cells in medial and dorsolateral prefrontal cortices and in the hippocampus (Figure S3) because the distribution of PV-positive cortical neurons, which represent a subset of GABAergic inhibitory neurons, is altered in some animal models of schizophrenia[40,44] and is thought to be a key abnormality underlying the pathogenesis of schizophrenia[45]. However, we did not observe any significant alterations in the distribution of PV-positive cells in *Zic2*$^{kd/+}$ cortices (Figure S3).

Our second key observation relates to those implying that abnormalities of the amygdala underlie the social behavior abnormalities in *Zic2*$^{kd/+}$ mice. The reduced aggressivity of *Zic2*$^{kd/+}$ mice was indicative of abnormal social behavior and we hypothesized that abnormalities of the amygdala were involved for a number of reasons. Firstly, it is well known that the amygdala is essential for controlling aggressive behaviors[46]. Also, lesions in the rat medial amygdala cause a reduction in aggressive behavior[47]. Adding further support, a recent study showed that the AHA and medial amygdala project into the hypothalamic aggression area (mediobasal hypothalamus), which plays a central role in the control of aggressive behavior[48]. These facts led us to hypothesize that the reduced aggressivity in *Zic2*$^{kd/+}$ mice is related to the altered morphology of AHA. However, there have been limited studies focusing on the role of AHA in aggressive behavior. Therefore, further investigation of the amygdalar abnormalities in *Zic2*$^{kd/+}$ mice would contribute to our understanding of the neural circuits controlling aggressive behavior.

The molecular mechanism of developmental disturbances that lead to the cholinergic neuronal loss and amygdalar dysgenesis remains elusive. As one interpretation, these abnormalities may reflect a milder representation of the HPE-like abnormality[8] and cortical dysgenesis partly as a result of the abnormal *Zic2*-expressing meningeal progenitor cells[11] in *Zic2*$^{kd/kd}$ mice. In terms of forebrain cholinergic neuron development, we found that the p75-expressing cholinergic progenitor neurons in the prospective medial septum and diagonal band are missing in *Zic1*/*Zic3* compound mutant mice[49]. Since the structure and function of the vertebrate Zic family of proteins is highly conserved[3], Zic2 might function to expand the medial forebrain cholinergic neural progenitor cells by inhibiting their exit from the proliferating cell cycle in a manner analogous to that in the *Zic1*/*Zic3* compound mutant mice[49].

Resequencing analysis of *Zic2* in Japanese patients with schizophrenia revealed three novel nonsynonymous mutations in *ZIC2*. Functional analysis of these mutations in the *Zic2*$^{kd/+}$ mouse model of schizophrenia indicated that the R409P mutation results in severe loss-of-function. We showed that the transcriptional activation capacity of the Zic2-R409P protein was about 20% that of the wild-type protein; which corresponds to the decreased protein production from the *Zic2*^{kd} allele shown previously[8]. This finding in turn validates *Zic2*$^{kd/+}$ mice as an animal model of the R409P mutation in schizophrenia. The patient with the R409P mutation was diagnosed with residual-type schizophrenia.

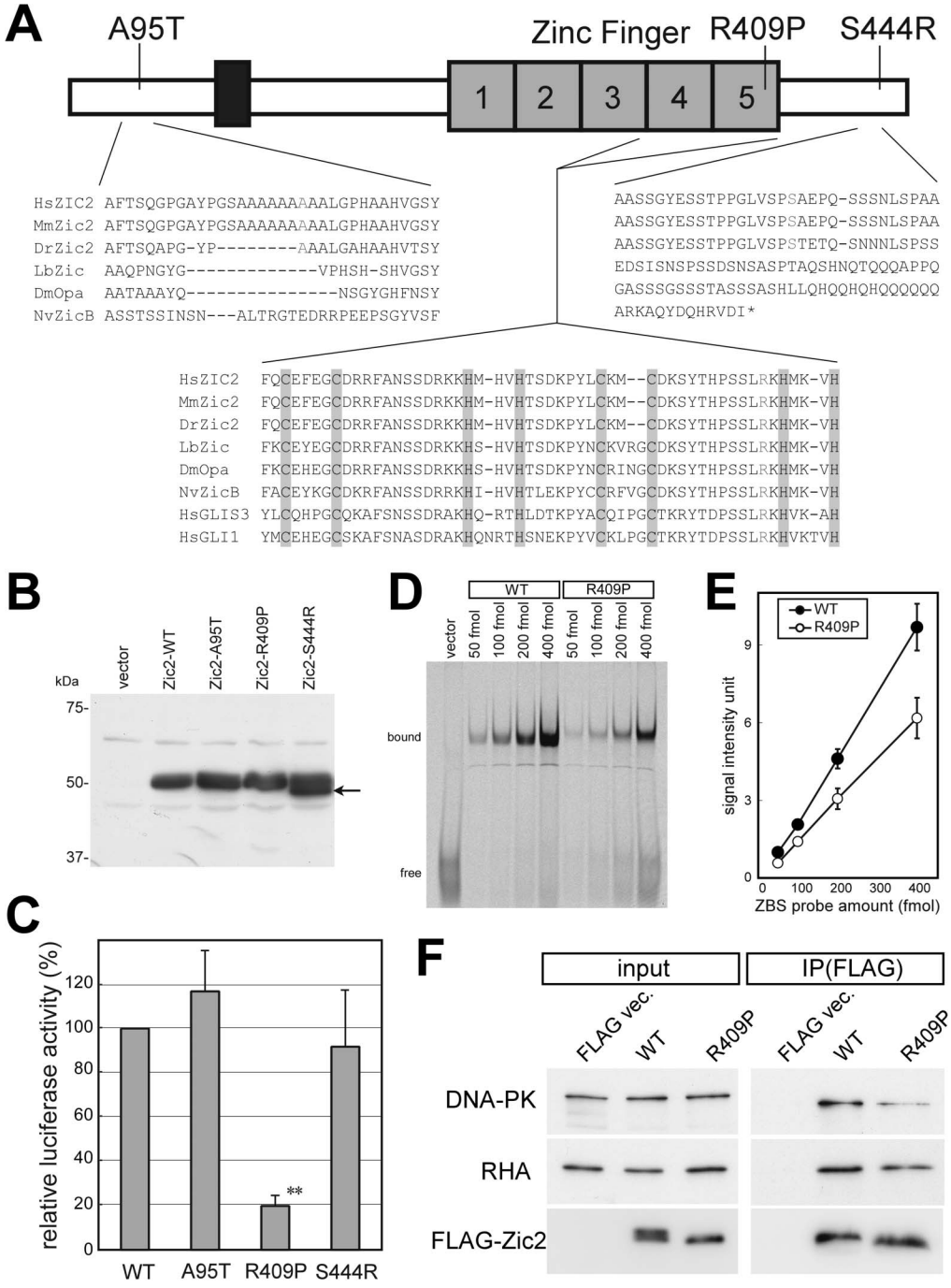

Figure 6 | Properties of ZIC2 variants found in schizophrenia patients. (A) Structure of the ZIC2 protein. Gray boxes with numbers indicate C2H2 motifs in the zinc finger domain of ZIC2. The positions of the A95T, R409P, and S444R mutations are indicated. Multiple alignments of the flanking regions of three mutations are indicated along with the reference sequences. Shaded characters show conserved cysteine and histidine residues in the C2H2 zinc fingers. Black box indicates an evolutionary conserved domain (ZOC, Zic-Opa-Conserved) domain. Gray characters indicate the mutated residues and the corresponding residues in other species (Hs, *Homo sapiens* [human]; Mm, *Mus musculus* [mouse]; Dr, *Danio rerio* [zebrafish]; Lb, *Loligo breekeri* [squid]; Dm, *Drosophila melanogaster* (fly); Nv, *Nematostella vectensis* [sea anemone]). (B) Immunoblotting of mouse wild-type Zic2 and Zic2 variants. NIH3T3 cells were transfected with the FLAG-tag expression plasmids. The Zic2 proteins were detected by the anti-FLAG antibody. Arrow indicates the fast migrating component in FLAG-Zic2-S444R. (C) NIH3T3 cells were transfected with a Zic2-responsive luciferase reporter vector together with a vector expressing wild-type FLAG-Zic2 (WT), or the FLAG-Zic2-A95T, -R409P, -S444R mutant proteins. All luciferase activities were normalized to the activities of the co-transfected elongation factor 1 promoter-driven Renilla luciferase. The means ± SEM of three independent experiments of three samples each are shown. (D) Gel mobility shift assay. IRD-labeled target DNAs were incubated with partially purified FLAG-Zic2-WT or FLAG-Zic2-R409P proteins expressed in 293T cells. The probes and the amount are indicated at the top. (E) Quantification of the gel shift assay result. Data are presented as means ± SEM. There were statistically significant differences between the FLAG-Zic2-WT and FLAG-Zic2-R409P-bound DNA probes at each dose (50 fmol, $P < 0.001$; 100 fmol, $P = 0.0022$; 200 fmol, $P = 0.012$; and 400 fmol, $P = 0.0089$). (F) FLAG-Zic2-WT or FLAG-Zic2-R409P expressed in 293T cells were immunoprecipitated with the anti-FLAG antibody. Proteins in the input cell lysates (input) and immunoprecipitates (IP) were analyzed by immunoblotting using anti-DNA-PK, anti-RHA, and anti-FLAG antibodies. There was a decrease in the amount of co-precipitated DNA-PK in FLAG-Zic2-R409P immunoprecipitates compared to those from FLAG-Zic2-WT, despite comparable amounts of FLAG-Zic2-R409P and FLAG-Zic2-WT.

Table 3 | Comparison of the morphological and behavioral features of *Zic2* kd/+ with those of other typical schizophrenia model mice.

	Lateral ventricular volume	Anxiety	Novelty induced activity	Working memory	PPI	Social recognition	R-I aggression	Social interaction
Zic2 kd/+	↑	=	↑	↓	↓	=	↓	=
DISC1-DN	↑	=	↑	=	↓	-	-	=
NRG1-TM	-	=	↑	=	↓	↓	↑	=
PV-ErbB4-/-	-	-	↑	↓	↓	-	-	-

Dominant negative *Disc* transgenic (DISC1-DN) and *Nrg1* transmembrane knockout (NRG1-TM) results summary is based on [20]. Conditional knockout of *Erbb4* in PV-positive interneuron (PV-ErbB4-/-) is based on [39]. ↑, increased relative to WT; ↓, decreased relative to WT; =, no difference; -, not reported.

Many studies have investigated the *ZIC2* mutations in patients with HPE. A recent meta-analysis study of previously published results showed that the vast majority of *ZIC2* mutations (98%) cause significant loss-of-function[7]. This suggests that HPE is caused by severely impaired function of *ZIC2*. Interestingly, only the very few cases (three families), in which the function of *ZIC2* was shown to be null, included two independent parents with normal brain imaging despite the identification of *ZIC2* missense mutations (Q36P or D152F)[7]. Together with these results, our findings raise the possibility that mildly impaired ZIC2 function does not result in HPE, but in psychiatric illnesses.

In summary, behavioral and morphological phenotypes in $Zic2^{kd/+}$ mice were reminiscent of those of schizophrenia. Additionally, the detection of rare, but significantly defective, missense mutations in patients with schizophrenia suggests that further analysis of *ZIC2* in neuropsychiatric patients is meaningful. Since this study focused on missense mutations, there still remains the possibility that mutations in introns and/or flanking regions that provoke partial loss of function are associated with schizophrenia.

Methods

Animals. Animal experiments were approved by the Animal Experiment Committee of the RIKEN Brain Science Institute (approval no. H22-EP068), and the mice were maintained by the institute's Research Resource Center. Mutant mice heterozygous for the $Zic2^{kd}$ allele ($Zic2^{kd/+}$) were described previously[8,9,12]. $Zic2^{kd}$ was generated by the insertion of the neomycin resistant cassette into an intron of mouse *Zic2*, resulting in the 20% of the wild-type allele[8], and were maintained in C57BL/6J background.

Behavioral tests. Home cage activity measurement, open field test, classical fear conditioning, Y-maze test were done as described[50,51].

Resident-intruder test. Group-reared mice were kept in isolation for 5 days before the test. The test was carried out in a dark phase (0:30 to 2:30) in a chamber that keeps the cage under dim (infrared) light at 25°C. Video recording from two opposite directions was initiated once the intruder mice had been gently placed in a vacant spot in the cage of the resident mice. The behaviors of the resident mouse were recorded for 10 min. The duration and number of times the resident mice spent sniffing, in active contact with, and in pursuit and attack with the intruder mice were measured by observers who were blinded to the genotypes of the mice.

Social dominance tube test. A wild type and a $Zic2^{kd/+}$ mice were placed in a head-to-head position first at the opposite ends of a clear plexiglass tube (3.4 cm inner diameter, 30 cm in length) in which two shutter plates were inserted at a distance of 13 cm from each end. The tests were begun by removing the shutters and ended when one mouse completely retreated from the tube. The mouse that retreated first was designated as the loser, and the remaining mouse was judged as the winner. The maximal test time was set to 2 min.

Magnetic resonance imaging (MRI) based volumetric analysis. MRI images of the adult male mice were acquired by subjecting anesthetized mice to an MRI scan using a vertical bore 9.4-T Bruker AVANCE 400WB imaging spectrometer (Bruker BioSpin, Rheinstetten, Germany). Animals were anesthetized with 3% and 1.5% isoflurane in air (2 L/min flow rate) for induction and maintenance, respectively. MRI images were obtained by using the FISP-3D protocol of Paravision software 5.0, by setting the following parameter values: Effective TE = 4.0 ms, TR = 8.0 ms, Flip angle = 15 degree, Average number = 5, Acquisition Matrix = 256 × 256 × 256, FOV = 25.6 × 25.6 × 25.6 mm. Manual measurements were made on the 3-dimensional (3D) MRI data to calculate total brain volume, hippocampus volume and lateral ventricle volume using the InsightITK-Snap software[52]. Regional volumetric changes were measured by voxel-based morphometry (VBM) using the Statistical Parametric Mapping (SPM) software package (http://www.fil.ion.ucl.ac.uk/spm/software/) for MATLAB (Mathworks, Natick, MA, USA) for pilot survey (data not shown).

Histology and immunostaining. Histological examination was done as described[9]. For the morphometric analysis, serial coronal sections were prepared, and analyzed at the following positions: +0.74 to +1.10 for the septum, diagonal band, striatum and the motor cortex; −0.34 to −0.82 for the substantia innominata, the basal nucleus of the Meynert, and the somatosensory cortex [anterior(+) to posterior(−) distance (mm) from bregma according to Paxinos et al.[53]]. The sections were stained with cresyl violet or by utilizing endogenous acetylcholine esterase activity[54] for histological examination.

Immunostaining was performed as previously described[55]. The primary antibodies were rabbit mouse anti-choline acetyltransferase (ChAT) polyclonal antibody (Chemicon, Temecula, CA, USA), mouse monoclonal anti-parvalbumin (PV) (Sigma, St. Louis, MO, USA), and rabbit anti-pan-Zic antibodies[10].

Resequencing analysis of *ZIC2* in human subjects. We performed resequencing analysis of *ZIC2* in 278 patients with schizophrenia who were of Japanese descent. The diagnosis of schizophrenia including the samples below was made on the basis of Diagnostic and Statistical Manual of Mental Disorders criteria (DSM-IV), by at least two expert psychiatrists. We then determined the allele frequencies of detected mutations using an expanded sample panel of schizophrenia patients (967 subjects: 457 men, 510 women; mean age 47.3 ± 13.8 [SD] years) and 1060 controls (502 men, 558 women; mean age 47.7 ± 13.6 years) who were documented as being free of mental disorders following brief interviews by expert psychiatrists. Our recruitment of schizophrenia and control subjects did not involve structured or semi-structured instruments. This study was approved by the ethics committees of RIKEN.

Protein-coding regions and exon/intron boundaries within the *ZIC2* gene were screened for polymorphisms by direct sequencing of PCR products using the BigDye Terminator v3.1 Cycle Sequencing kit (Applied Biosystems, Foster City, CA, USA) and the ABI PRISM 3730xl Genetic Analyzer (Applied Biosystems).

Molecular and functional analysis. Mouse *Zic2* variants that have the same missense mutations as the human *ZIC2* nonsynonymous mutations ($Zic2^{A95T}$ for $ZIC2^{A95T}$, $Zic2^{R408P}$ for $ZIC2^{R409P}$, and $Zic2^{S443R}$ for $ZIC2^{S444R}$) were generated by PCR[56] using pEFBOS-*Zic2*[31] or pcDNA3-HA-*Zic2* as templates. Hereinafter, we refer to them as *Zic2*-A95T ($Zic2^{A95T}$), *Zic2*-R409P ($Zic2^{R408P}$) and *Zic2*-S444R ($Zic2^{S443R}$), respectively. Expression plasmids for these wild-type *Zic2* and *Zic2* variants were constructed pcDNA3.1 (Invitrogen, Carlsband, CA, USA) and pCMVtag2 (Stratagene, La Jolla, CA, USA). pGL4-ZBS was constructed by inserting a mouse genomic DNA clone containing Zic2-binding sequences (Ishiguro et al., unpublished) into pGL4 (Promega, Madison, WI, USA). Cell culture, transfection, immunoblot analysis. luciferase reporter assay, gel shift assay, and immunoprecipitation were performed as previously described[31,33].

Statistical analysis. Parametric data were analyzed by using the two-sided Student's *t*-test (t-test) and non-parametric data were analyzed by using the Mann–Whitney's *U*-test (U-test). The *P* values refer to the t-test, unless otherwise specified. We also used the repeated measure two-way analysis of variance (RMANOVA) or the chi-square test for homogeneity. Differences were defined as statistically significant when $P < 0.05$.

1. Aruga, J. *et al.* The mouse zic gene family. Homologues of the Drosophila pair-rule gene odd-paired.*J Biol Chem* **271**, 1043–1047 (1996).
2. Nagai, T. *et al.* The expression of the mouse Zic1, Zic2, and Zic3 gene suggests an essential role for Zic genes in body pattern formation. *Dev Biol* **182**, 299–313 (1997).
3. Aruga, J. The role of Zic genes in neural development. *Mol Cell Neurosci* **26**, 205–221 (2004).
4. Grinberg, I. & Millen, K. J. The ZIC gene family in development and disease. *Clin Genet* **67**, 290–296, doi:10.1111/j.1399-0004.2005.00418.x (2005).
5. Merzdorf, C. S. Emerging roles for zic genes in early development. *Dev Dyn* **236**, 922–940 (2007).
6. Brown, S. A. *et al.* Holoprosencephaly due to mutations in ZIC2, a homologue of Drosophila odd-paired. *Nat Genet* **20**, 180–183 (1998).

7. Solomon, B. D. *et al.* Mutations in ZIC2 in human holoprosencephaly: description of a Novel ZIC2 specific phenotype and comprehensive analysis of 157 individuals. *J Med Genet* **47**, 513–524 (2010).
8. Nagai, T. *et al.* Zic2 regulates the kinetics of neurulation. *Proc Natl Acad Sci U S A* **97**, 1618–1623 (2000).
9. Aruga, J., Inoue, T., Hoshino, J. & Mikoshiba, K. Zic2 controls cerebellar development in cooperation with Zic1. *J Neurosci* **22**, 218–225 (2002).
10. Inoue, T., Ota, M., Mikoshiba, K. & Aruga, J. Zic2 and Zic3 synergistically control neurulation and segmentation of paraxial mesoderm in mouse embryo. *Dev Biol* **306**, 669–684 (2007).
11. Inoue, T., Ogawa, M., Mikoshiba, K. & Aruga, J. Zic deficiency in the cortical marginal zone and meninges results in cortical lamination defects resembling those in type II lissencephaly. *J Neurosci* **28**, 4712–4725 (2008).
12. Ogura, H., Aruga, J. & Mikoshiba, K. Behavioral abnormalities of Zic1 and Zic2 mutant mice: implications as models for human neurological disorders. *Behav Genet* **31**, 317–324 (2001).
13. Freedman, R. Schizophrenia. *N Engl J Med* **349**, 1738–1749 (2003).
14. Ross, C. A., Margolis, R. L., Reading, S. A., Pletnikov, M. & Coyle, J. T. Neurobiology of schizophrenia. *Neuron* **52**, 139–153 (2006).
15. Jaaro-Peled, H., Ayhan, Y., Pletnikov, M. V. & Sawa, A. Review of pathological hallmarks of schizophrenia: comparison of genetic models with patients and nongenetic models. *Schizophr Bull* **36**, 301–313 (2010).
16. Steen, R. G., Mull, C., McClure, R., Hamer, R. M. & Lieberman, J. A. Brain volume in first-episode schizophrenia: systematic review and meta-analysis of magnetic resonance imaging studies. *Br J Psychiatry* **188**, 510–518 (2006).
17. Vita, A., De Peri, L., Silenzi, C. & Dieci, M. Brain morphology in first-episode schizophrenia: a meta-analysis of quantitative magnetic resonance imaging studies. *Schizophr Res* **82**, 75–88 (2006).
18. Ellison-Wright, I., Glahn, D. C., Laird, A. R., Thelen, S. M. & Bullmore, E. The anatomy of first-episode and chronic schizophrenia: an anatomical likelihood estimation meta-analysis. *Am J Psychiatry* **165**, 1015–1023 (2008).
19. Karayiorgou, M., Simon, T. J. & Gogos, J. A. 22q11.2 microdeletions: linking DNA structural variation to brain dysfunction and schizophrenia. *Nat Rev Neurosci* **11**, 402–416 (2010).
20. Desbonnet, L., Waddington, J. L. & Tuathaigh, C. M. Mice mutant for genes associated with schizophrenia: common phenotype or distinct endophenotypes? *Behav Brain Res* **204**, 258–273 (2009).
21. Jaaro-Peled, H. *et al.* Neurodevelopmental mechanisms of schizophrenia: understanding disturbed postnatal brain maturation through neuregulin-1-ErbB4 and DISC1. *Trends Neurosci* **32**, 485–495 (2009).
22. Kellendonk, C., Simpson, E. H. & Kandel, E. R. Modeling cognitive endophenotypes of schizophrenia in mice. *Trends Neurosci* **32**, 347–358 (2009).
23. Pineda-Alvarez, D. E., Dubourg, C., David, V., Roessler, E. & Muenke, M. Current recommendations for the molecular evaluation of newly diagnosed holoprosencephaly patients. *Am J Med Genet C Semin Med Genet* **154C**, 93–101 (2010).
24. Brown, L. Y. *et al.* Holoprosencephaly due to mutations in ZIC2: alanine tract expansion mutations may be caused by parental somatic recombination. *Hum Mol Genet* **10**, 791–796 (2001).
25. Orioli, I. M. *et al.* Identification of novel mutations in SHH and ZIC2 in a South American (ECLAMC) population with holoprosencephaly. *Hum Genet* **109**, 1–6 (2001).
26. Dubourg, C. *et al.* Molecular screening of SHH, ZIC2, SIX3, and TGIF genes in patients with features of holoprosencephaly spectrum: Mutation review and genotype-phenotype correlations. *Hum Mutat* **24**, 43–51 (2004).
27. Roessler, E. *et al.* The full spectrum of holoprosencephaly-associated mutations within the ZIC2 gene in humans predicts loss-of-function as the predominant disease mechanism. *Hum Mutat* **30**, E541–554 (2009).
28. Aruga, J. *et al.* A wide-range phylogenetic analysis of Zic proteins: implications for correlations between protein structure conservation and body plan complexity. *Genomics* **87**, 783–792 (2006).
29. Pavletich, N. P. & Pabo, C. O. Crystal structure of a five-finger GLI-DNA complex: new perspectives on zinc fingers. *Science* **261**, 1701–1707 (1993).
30. Ramensky, V., Bork, P. & Sunyaev, S. Human non-synonymous SNPs: server and survey. *Nucleic Acids Res* **30**, 3894–3900 (2002).
31. Mizugishi, K., Aruga, J., Nakata, K. & Mikoshiba, K. Molecular properties of Zic proteins as transcriptional regulators and their relationship to GLI proteins. *J Biol Chem* **276**, 2180–2188 (2001).
32. Mizugishi, K. *et al.* Myogenic repressor I-mfa interferes with function of Zic family proteins. *Biochem Biophys Res Comm* **320**, 233–240 (2004).
33. Ishiguro, A., Ideta, M., Mikoshiba, K., Chen, D. J. & Aruga, J. ZIC2-dependent transcriptional regulation is mediated by DNA-dependent protein kinase, poly(ADP-ribose) polymerase, and RNA helicase A. *J Biol Chem* **282**, 9983–9995 (2007).
34. Arguello, P. A. & Gogos, J. A. Modeling madness in mice: one piece at a time. *Neuron* **52**, 179–196 (2006).
35. Stefansson, H. *et al.* Neuregulin 1 and susceptibility to schizophrenia. *Am J Hum Genet* **71**, 877–892 (2002).
36. O'Tuathaigh, C. M. *et al.* Phenotypic characterization of spatial cognition and social behavior in mice with 'knockout' of the schizophrenia risk gene neuregulin 1. *Neuroscience* **147**, 18–27 (2007).
37. Pletnikov, M. V. *et al.* Inducible expression of mutant human DISC1 in mice is associated with brain and behavioral abnormalities reminiscent of schizophrenia. *Mol Psychiatry* **13**, 173–186, 115 (2008).
38. Hikida, T. *et al.* Dominant-negative DISC1 transgenic mice display schizophrenia-associated phenotypes detected by measures translatable to humans. *Proc Natl Acad Sci U S A* **104**, 14501–14506 (2007).
39. Wen, L. *et al.* Neuregulin 1 regulates pyramidal neuron activity via ErbB4 in parvalbumin-positive interneurons. *Proc Natl Acad Sci U S A* **107**, 1211–1216, doi:10.1073/pnas.0910302107 (2010).
40. Shen, S. *et al.* Schizophrenia-related neural and behavioral phenotypes in transgenic mice expressing truncated Disc1. *J Neurosci* **28**, 10893–10904 (2008).
41. Chen, X. W. *et al.* DTNBP1, a schizophrenia susceptibility gene, affects kinetics of transmitter release. *J Cell Biol* **181**, 791–801 (2008).
42. Picciotto, M. R., Alreja, M. & Jentsch, J. D. in *Neuropsychopharmacology, the fifth generation of progress* (eds K. L. Davis, D. Charney, J. T. Coyle, & C. Nemerroff) 3–14. (Lippincott Williams & Wilkins, 2002).
43. Ross, R. G. *et al.* Research review: Cholinergic mechanisms, early brain development, and risk for schizophrenia. *J Child Psychol Psychiatry* **51**, 535–549 (2010).
44. Lodge, D. J., Behrens, M. M. & Grace, A. A. A loss of parvalbumin-containing interneurons is associated with diminished oscillatory activity in an animal model of schizophrenia. *J Neurosci* **29**, 2344–2354 (2009).
45. Gonzalez-Burgos, G., Hashimoto, T. & Lewis, D. A. Alterations of cortical GABA neurons and network oscillations in schizophrenia. *Curr Psychiatry Rep* **12**, 335–344.
46. Bear, M. F., Connors, B. W. & Paradiso, M. A. in *Neuroscience, exploring the brain* 572–583. (Lippincott Williams & Wilkins, 2007).
47. Vochteloo, J. D. & Koolhaas, J. M. Medial amygdala lesions in male rats reduce aggressive behavior: interference with experience. *Physiol Behav* **41**, 99–102 (1987).
48. Toth, M., Fuzesi, T., Halasz, J., Tulogdi, A. & Haller, J. Neural inputs of the hypothalamic "aggression area" in the rat.*Behav Brain Res* **215**, 7–20 (2010).
49. Inoue, T., Ota, M., Ogawa, M., Mikoshiba, K. & Aruga, J. Zic1 and Zic3 regulate medial forebrain development through expansion of neuronal progenitors. *J Neurosci* **27**, 5461–5473 (2007).
50. Katayama, K. *et al.* Slitrk1-deficient mice display elevated anxiety-like behavior and noradrenergic abnormalities. *Mol Psychiatry* **15**, 177–184, doi:10.1038/mp.2008.97 (2010).
51. Araya, R. *et al.* Loss of M5 muscarinic acetylcholine receptors leads to cerebrovascular and neuronal abnormalities and cognitive deficits in mice. *Neurobiol Dis* **24**, 334–344 (2006).
52. Yushkevich, P. A. *et al.* User-guided 3D active contour segmentation of anatomical structures: significantly improved efficiency and reliability. *Neuroimage* **31**, 1116–1128 (2006).
53. Paxinos, G. & Franklin, K. B. J. *The mouse brain in stereotaxic coordinates.* 2 edn, (Academic Press, 2001).
54. Vincent, S. R. in *Experimental neuroanatomy* (ed J. P. Bolam) Ch. 7, (Oxford University Press, 1992).
55. Aruga, J., Nozaki, Y., Hatayama, M., Odaka, Y. S. & Yokota, N. Expression of ZIC family genes in meningiomas and other brain tumors. *BMC Cancer* **10**, 79 (2010).
56. Fisher, C. L. & Pei, G. K. Modification of a PCR-based site-directed mutagenesis method. *Biotechniques* **23**, 570–571, 574 (1997).

Acknowledgments

We thank the members of Aruga Laboratory for valuable discussions, Naoko Yamada, Yoshie Ito and Ryoko Takei for technical assistance, and Katsuhiko Mikoshiba for continuous encouragement of our Zic biology project. This work was supported by RIKEN BSI Funds and by a Grant-in-Aid for Scientific Research from the Ministry of Education, Culture, Sports, Science and Technology of Japan. A part of this study is the result of "Development of biomarker candidates for social behavior" carried out under the Strategic Research Program for Brain Sciences by the Ministry of Education, Culture, Sports, Science and Technology of Japan.

Author contributions

M.H. and A.I. characterized the ZIC2 variants. Y.I., T.T. and T.Y. performed the resequencing analysis. A.I., N.T., K.S. Y.S.O., K.Y. and J.A. performed the behavioral analysis. K.S. performed the MRI analysis. Y. N. and J.A. performed the histological analysis. M.H., A.I., K.Y., T.Y. and J.A. wrote the manuscript.

Additional information

Supplementary Information accompanies this paper at http://www.nature.com/scientificreports

Competing financial interests: The authors declare that there are no conflicts of interest associated with the present study.

How to cite this article: Hatayama, M. *et al. Zic2* hypomorphic mutant mice as a schizophrenia model and *ZIC2* mutations identified in schizophrenia patients *Sci. Rep.* **1**, 16; DOI:10.1038/srep00016 (2011).